

If $r^2 = \gamma d$, the Coulomb interaction is independent of the density, which is the usual situation. Then

$$E/N = 2\pi\sqrt{d}/\sqrt{\gamma} + \pi^2/3\gamma d. \quad (21)$$

If $\lambda \neq 0$, use the expansion for φ ,

$$\varphi' \approx -\frac{\pi^2}{r^2} \frac{1}{\sinh^2(x/\pi r)} - \frac{2\pi}{rL}, \quad (22)$$

and find

$$\begin{aligned} v_0 \rightarrow v_0' &= \lambda^2 v_0, \\ v_1 \rightarrow v_1' &= \lambda^2 v_1 + \frac{2\lambda\pi^2(\lambda-1)}{r^2} \frac{1}{\sinh^2(\pi x/r)}. \end{aligned} \quad (23)$$

Then the energy per particle is

$$\frac{E}{N} \rightarrow \frac{2\pi\lambda d}{r} + \frac{\lambda^2\pi}{3r^2} = \frac{2\pi\lambda\sqrt{d}}{\sqrt{\gamma}} + \frac{\lambda^2\pi}{3\gamma d}. \quad (24)$$

In the opposite situation, where $r \gg L$, one recovers the case discussed in Ref. 1.

In order to obtain more explicit results, go one step further and consider the limit $\lambda, r \rightarrow 0, \lambda/r = q/d$. Then

$$V_0' \sim -4\pi q^2 |x| + 4\pi^2 q^2 x^2/L. \quad (25)$$

It is easier to proceed from the wave function di-

rectly:

$$\begin{aligned} \psi^\lambda &= \exp\{-[(|x| - \frac{1}{2}L)^2 - (\frac{1}{2}L)^2]\} \\ &(0 < |x| < L). \end{aligned} \quad (26)$$

One then finds

$$V_1' \sim 4\pi q d^{-1/2} \delta(x), \quad (27)$$

and

$$E/N \sim 2\pi q d^{1/2} + \pi^2 q^2/3d. \quad (28)$$

Using the techniques developed for the thermodynamics of the classical partition function, one may calculate the normalization and correlation in the ground state. These results will be reported in a subsequent publication.

*Work supported in part by National Science Foundation under Grant No. CP38905.

†Permanent address: Physics Department, University of Utah, Salt Lake City, Utah 84112.

¹B. Sutherland, *Phys. Rev. A* **4**, 2019 (1971).

²B. Sutherland, unpublished.

³E. T. Whittaker and G. N. Watson, *A Course of Modern Analysis* (Cambridge Univ. Press, Cambridge, England, 1927). In particular, my Eq. (5) is given as an exercise on page 446.

⁴Whittaker and Watson, Ref. 3, Chap. 21.

Neutral Injection Heating Experiments on the Oak Ridge Tokamak Device*

L. A. Berry, J. D. Callen, R. J. Colchin, G. G. Kelley, J. F. Lyon, and J. A. Rome
Oak Ridge National Laboratory, Oak Ridge, Tennessee 37830

(Received 11 December 1974)

Proton heating varying from 10 to 40% as plasma density is decreased has been observed as a result of energetic H^0 beam injection parallel to the discharge current on the ORMAK device. The change in ion temperature agrees with a theoretical heating calculation in both density scaling and magnitude. In contrast to the results reported for the ATC device at Princeton Plasma Physics Laboratory, no measurable heating was observed for an antiparallel beam.

It has been recognized for some time that supplementary heating is necessary to raise the temperature of an Ohmically heated tokamak plasma to the level required for fusion experiments.¹ A promising heating method is that of injecting an energetic neutral beam.² Experiments at Oak Ridge National Laboratory,³ Princeton University,^{4,5} and Culham Laboratory⁶ have demonstrated that this technique can produce experimentally significant ion heating. We have extended those results and isolated the component of the heating due directly to the beam by measuring the varia-

tion in ion temperature as a function of electron density. We find that the calculated heating agrees with the experimental data both in magnitude and in the scaling with electron density.

Detailed measurements of discharge parameters in the ORMAK device have been reported in previous articles.⁷⁻⁹ The machine geometry and discharge characteristics that are relevant to the experiments described below are given in Table I. Thomson scattering, 2-mm microwave interferometry, and charge-exchange neutral analysis were used for making the measurements of elec-

TABLE I. ORMAK parameters.

Major radius	80 cm
Minor radius	23 cm
Discharge current	95 kA
Discharge voltage	2.5–3.5 V
Toroidal field	18 kG
Average electron density	$(1-2.5) \times 10^{13}/\text{cm}^3$
Central electron temperature	400–1000 eV
Average electron temperature	200–300 eV
Central ion temperature	160–250 eV
Central neutral density	$\sim (1-2) \times 10^8/\text{cm}^3$

tron temperature, electron density, and ion temperature and neutral density, respectively.

The neutral-beam injectors used in the heating experiments are each capable of delivering more than 100 kW in beam power to the discharge for times of up to 0.2 sec. Detailed characteristics of their operation have been presented elsewhere.¹⁰ Two injectors have been installed. They are aimed approximately tangential to (8 cm inside) the magnetic axis and are oppositely arranged. One injector produces a H⁰ beam parallel to the plasma current (coinjection) and the other produces an antiparallel beam (counterinjection). The roles of the injectors are routinely interchanged by reversing the discharge current direction.

The timing of a typical experiment is shown in Fig. 1. A large voltage ionizes the fill hydrogen gas and drives the rapid initial current rise. The desired toroidal current is reached after about 15 msec, and then held nearly constant by a feedback system until the experiment is terminated, usually because the iron core has begun to saturate. The discharge current is clamped at this time and undergoes an inductive decay. Some time after the plasma is well established, the neutral beam is turned on, reaching full current in about 10 msec for this case.

The response of the ion temperature and line-averaged electron density to a coinjected beam is shown in Fig. 2. The mechanism responsible for the density increase that is apparent in the figure is not understood. The increase is too large, however, to be accounted for by plasma ionization of neutral gas streaming from the source,

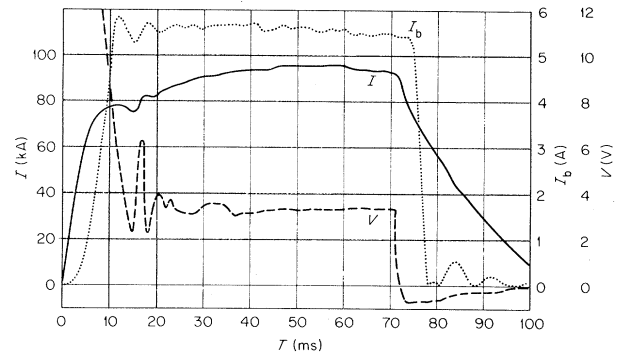


FIG. 1. Plasma current (I), one-turn voltage (V), and extracted ion beam current (I_b).

additional particle refluxing induced by increased wall bombardment, or direct accumulation of the trapped beam. These conclusions are based on, respectively, the observation of constant density with normal source operation but no extracted beam, spectroscopic measurements of L_β and C III line intensities, and theoretical estimates of confined-beam densities that are about a factor of 4 lower than the measured density increase.

The presence of this observed density increase complicates the experimental analysis as can be seen in the equation¹¹

$$\frac{\Delta T_i}{T_i} = \frac{P_{inj,i}}{P_{ei}} + \frac{\Delta n_e}{n_e} \left(1 + n_e \frac{\partial \ln \tau_{Ei}}{\partial n_e} \right) + \frac{\Delta n_0}{n_0} \left(n_0 \frac{\partial \ln \tau_{Ei}}{\partial n_0} \right) \left(\frac{3}{2} - T_i \frac{\partial \ln \tau_{Ei}}{\partial T_i} \right)^{-1}, \quad (1)$$

which gives an estimate of the ion temperature increase ΔT_i in terms of the injected beam power

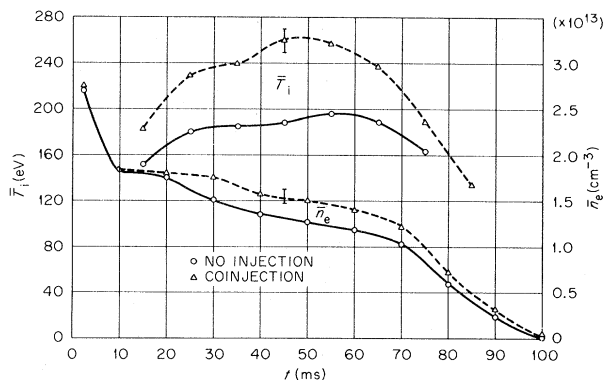


FIG. 2. Plasma response to H⁰ injection. The average electron density was measured by a 2-mm microwave interferometer and the proton temperature by analysis of charge-exchange neutral signals.

that is deposited in the ions $P_{inj,i}$, the unperturbed collisional electron-ion power transfer P_{ei} , and any associated changes in the plasma density Δn_e and neutral density Δn_0 . Allowance is also made for changes in the ion energy lifetime τ_{Ei} . The presence of the Δn_e and Δn_0 terms in the numerator allow for the possibility of an ion temperature increase that is not directly associated with the injected beam but is rather a secondary effect. From a computational point of view it should be noted that (1) all terms in the above equation are volume averages using appropriate radial profiles; (2) it is a perturbation calculation valid for small ΔT_i ; and (3) all energy components in the injected beam are treated independently.

The separation of beam-induced heating from that which may be associated with an electron density perturbation is accomplished by measuring the ion temperature as a function of electron density for discharges both with and without neutral injection, as shown in Fig. 3. Now the ion temperature change can be examined at constant density, and we see that almost all of the increase for coinjection is due directly to beam heating. The decrease in ΔT_i with increasing n_e is due to the fact that $P_{inj,i}$ does not increase as rapidly with density as P_{ei} , which is locally proportional to n_e^2 .

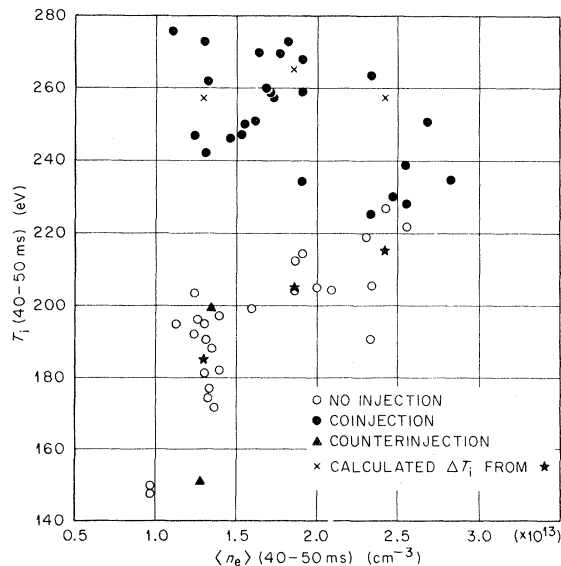


FIG. 3. Proton temperatures as a function of average electron density measured at 40–50 msec in the “flat” portion of the current pulse. The temperature is obtained by analyzing the charge-exchange neutral spectrum in the range 500–1000 eV.

The agreement between the coinjection experimental points and the theoretical values for ΔT_i can be seen in Fig. 3. Taking three average no-injection points spanning the density range as typical “no-injection” starting points (designated by stars), the ΔT_i 's expected from the beam power input alone have been calculated from Eq. (1) with the following assumptions: (1) $\Delta n_e = 0$ since the comparison is made at constant plasma density; (2) the Δn_0 term is neglected since Δn_0 is proportional to Δn_e ($n_0 \sim n_e^{-1}$ in ORMAK⁸); and (3) $T_i \times \partial \ln \tau_{Ei} / \partial T_i$ is neglected since it is small¹¹ (magnitude < 0.2) compared to $\frac{3}{2}$.

In contrast with coinjection, the typical counterinjection points in Fig. 3 fall within the spread of the no-injection points, indicating little net ion heating. Also, both injectors together give about the same ion heating as coinjection alone. Calculations show that with counterinjection most of the beam power should be lost by pitch-angle scattering into unconfined “banana” orbits. Measurements of the perpendicular energy spectrum of the fast ions support this prediction, but indicate that some power transfer to the ions ($\sim \frac{1}{2}$ to $\frac{1}{5}$ of the coinjected value) must have occurred. Even this reduced heating should result in an observable ion temperature increase. The fact that no significant temperature rise is seen in general is probably because of the offsetting effects of somewhat lowered electron density, increased impurity levels, and decreased plasma stability that we often observe with counterinjection.¹² Although significant in present experiments, the counterinjection particle loss by unconfined banana orbits should become unimportant for larger machine sizes and higher poloidal fields since this effect scales as the fast-ion poloidal gyroradius over the plasma radius.

In contrast, counterinjection ion heating has been reported on the ATC device at Princeton Plasma Physics Laboratory, although at somewhat reduced efficiency compared to coinjection heating.¹³ This difference between the ORMAK and ATC counterinjection results is most likely due to two factors: (1) The velocity-space region corresponding to unconfined fast-ion orbits in ATC is both smaller and less accessible; and (2) the ATC injection energy is lower, producing a larger fraction of fast ions energetically prevented from becoming unconfined, as well as permitting more efficient ion heating. In ATC, charge exchange of fast ions, the dominant power-loss mechanism, reduces the importance of the loss region for counterinjection and lowers

the ion heating efficiency for both beam directions.

While the bulk of this Letter has concentrated on ion heating, Thomson-scattering measurements indicate that electron temperature increases as a result of coinjection and in some cases decreases for counterinjection. There are changes in the temperature profiles at the same time that complicate the separation of beam-produced heating from that which is possibly due to a redistribution of the Ohmic heating current.

Our study supports the continued use of neutral beams for plasma heating. This confidence is based on (1) almost all of the ion heating we observe is due directly to the injected beam; (2) the measured and calculated ion temperature increases for coinjection are in agreement; and (3) a basic understanding of the present relative inefficiency for counterinjection.

The authors gratefully acknowledge the important contributions of their co-workers. P. H. Edmonds and W. R. Wing were responsible for machine operations, M. Murakami for laser Thomson scattering measurements, and J. F. Clarke for contributions to neutral injection heating theory. The ORMAK injectors were developed and installed by the Oak Ridge National Laboratory Thermonuclear Division Plasma Heating Department.

*Research sponsored by the Energy Research and Development Administration under contract with the Union Carbide Corporation.

¹I. N. Golovin, Yu. N. Dnestrovskii, and D. P. Kostomarov, in *Proceedings of the British Nuclear Energy*

Society Conference on Nuclear Fission Reactors, Culham Laboratory, 1969 (United Kingdom Atomic Energy Authority, Culham, England, 1970).

²G. G. Kelley, O. B. Morgan, L. D. Stewart, W. L. Stirling, and H. K. Forsen, *Nucl. Fusion* **12**, 169 (1972).

³C. F. Barnett *et al.*, in *Proceedings of the Sixth European Conference on Controlled Fusion and Plasma Physics, Moscow, U.S.S.R., 1973* (U.S.S.R. Academy of Sciences, Moscow, 1973).

⁴R. A. Ellis *et al.*, in *Proceedings of the Sixth European Conference on Controlled Fusion and Plasma Physics, Moscow, U.S.S.R., 1973* (U.S.S.R. Academy of Sciences, Moscow, 1973).

⁵K. Bol *et al.*, *Phys. Rev. Lett.* **32**, 661 (1974).

⁶J. G. Cordey *et al.*, to be published.

⁷G. G. Kelley *et al.*, in *Proceedings of the Third International Symposium on Toroidal Plasma Confinement, Garching, Germany, 1973* (Max Planck Institut für Plasmaphysik, Garching, Germany, 1973).

⁸L. A. Berry, J. F. Clarke, and J. T. Hogan, *Phys. Rev. Lett.* **32**, 362 (1974).

⁹M. Murakami, W. R. Wing, and P. H. Edmonds, to be published.

¹⁰L. D. Stewart *et al.*, in *Proceedings of the Third International Symposium on Toroidal Plasma Confinement, Garching, Germany, 1973* (Max Planck Institut für Plasmaphysik, Garching, Germany, 1973).

¹¹J. D. Callen, R. J. Colchin, R. H. Fowler, D. G. McAlees, and J. A. Rome, in *Proceedings of the International Conference on Plasma Physics and Controlled Nuclear Fusion Research, Tokyo, Japan, 11-15 November 1974* (to be published), Paper No. CN-33/A 16-3, and references cited therein.

¹²L. A. Berry *et al.*, in *Proceedings of the International Conference on Plasma Physics and Controlled Nuclear Fusion Research, Tokyo, Japan, 11-15 November 1974* (to be published), Paper No. CN-33/A 5-2.

¹³K. Bol *et al.*, in *Proceedings of the International Conference on Plasma Physics and Controlled Nuclear Fusion Research, Tokyo, Japan, 11-15 November 1974* (to be published), Paper No. CN-33/A 4-1.

Extrinsic Electroabsorption: N Symmetry in GaP

R. S. Bauer and R. D. Burnham

Xerox Palo Alto Research Center, Palo Alto, California 94304

(Received 10 March 1975)

The field-dependent absorption of N in GaP is determined by a new method employing depletion-region modulation. To explain the line shape and the peak increase with \mathcal{E} , we propose a Franz-Keldysh-type mechanism. It is based on the field's permitting non-direct transitions, with an orientation dependence determined by the impurity symmetry. We deduce that N has the GaP X_1 symmetry, with masses $m_l = (1.35 \pm 0.1)m_0$ and $m_t = (0.175 \pm 0.01)m_0$.

The dependence of the optical constants on electric field strength has proven to be an important tool for studying solids. Its value depends on un-

derstanding the physics of both the measurement technique and the mechanism causing the solid's response to a field. For example, the develop-